Title
Wearable Assistive Hand Exoskeleton for Activities of Daily Living

Author
Harris, Morgan

Publication Date
2022

Peer reviewed|Thesis/dissertation

Wearable Assistive Hand Exoskeleton for Activities of Daily Living

By

MORGAN HARRIS

THESIS

Submitted in partial satisfaction of the requirements for the degree of

MASTER OF SCIENCE

in

Mechanical Engineering

in the

OFFICE OF GRADUATE STUDIES

of the

UNIVERSITY OF CALIFORNIA

DAVIS

Approved:

Jonathon Schofield, Chair

Iman Soltani Bozchalooi

Sanjay S. Joshi

Committee in Charge

2022

Table of Contents

Abstract

Stroke impacts over 795,000 people each year and 33% of survivors will suffer from significant motor impairments. 73-88% of stroke survivors experience upper limb impairments. This significantly decreases one's ability to perform many daily tasks and can substantially reduce their quality of life and independence. Robotic hand exoskeletons are devices that can move a human hand to achieve grasping motions. They have the potential to support those with hand motor impairments during activities of daily living (ADL); however, current devices are primarily designed for use in rehabilitative environments and have not been effectively translated for use in daily living. This work aims to develop and characterize the mechanical and electrical performance of a hand exoskeleton that can perform common hand grasps and has the potential to assist an impaired hand in ADL. Most current hand exoskeletons reported in literature are designed with only comfort and basic hand movements in mind. For example, many only actuate three digits, while others can only perform a whole-hand open/closed grasp. We planned to build an exoskeleton that can individually actuate all digits, complete multiple common grasps and therefore be more capable of assisting in various ADL. The goals of this work were to: 1) design a functional hand exoskeleton, 2) measure and characterize the force outputs, current draw, and power of the individual digits of the exoskeleton when worn on a mannequin hand, and 3) use manipulanda to characterize the exoskeleton's ability to complete nine common adult hand grasps utilized in activities of daily living.

1 Introduction

1.1 Goals & Scope

The overall goal of this research is to create a hand exoskeleton for individuals suffering stroke-related hand motor impairments that assists with digit flexion and extension to facilitate common hand grasps. The objectives of the work are as follows:

- Design a functional hand exoskeleton
- Explicitly quantify the force outputs, current draw and power of the individual digits of the exoskeleton when worn on a mannequin hand
- Characterize the exoskeleton's capabilities to assist in the grasping/manipulation of common household objects.

1.2 Literature Review

Nationally, over 795,000 people suffer from stroke each year [0]. The term 'healthy life lost' is equal to the sum of years of life lost due to premature mortality and years lived with disability [2]. At least 63% of healthy life lost due to stroke-related death and disability affects people under the age of 70 [3]. Additionally, stroke is one of the leading causes of disability globally [4] and is among the top 10 causes of long-term physical disability [5]. There are two major disabilities that result from stroke: spasticity/muscle tone and hemiparesis, both of which can lead to hand motor impairment. Spasticity and muscle tone are abnormal muscle tightness due to prolonged muscle contraction, where the muscle remains contracted, and resists being stretched. They are relatively frequent consequences of stroke and have major impacts on daily function and quality of life [6]. Spasticity and muscle tone are quite common in stroke survivors, as 95% of patients experience mild to severe spasticity in their affected upper limb according to a study by the National Institute of Health [6]. It is an important disability to consider because if not treated with physical therapy in a timely fashion, it can cause pain in the limb, limb muscle atrophy, joint contracture deformation and eventually limited joint mobility [7]. Hemiparesis is the partial paralysis of one side of the body that can affect the limb and facial muscles [8]. Chronic upper-extremity hemiparesis is most often caused by stroke and affects 55-75% of stroke survivors [9,10]. As a result, there is a strong likelihood of a reduction in dexterity and motor function. These are significant causes of disability following stroke [11]. Post stroke, hand impairment is typically classified as 'chronic' in survivors and manifests itself as a loss of finger strength, loss of dexterity and abnormal hand flexion [4]. Research has found that it leaves patients with an average of 36% reduction in maximum force produced by the affected hand [12]. These disabilities cause deficits in arm function which are associated with poor quality of life [9].

Reduction of arm function is directly associated with the inability to perform activities of daily living (ADL). ADL are skills acquired to manage one's basic physical needs [13]. They are considered vital, yet routine tasks that most healthy individuals can complete without additional assistance; therefore, the inability to perform essential ADL can result in unsafe conditions and poor quality of life [13]. Each year, 26% of survivors remain impaired in basic ADL one year post stroke [14]. The loss of independence of upper limb function contributes enormously to functional disability, affecting quality of life and

independence in basic and instrumental activities of daily living [15]. Thus, stroke impacts the ability of individuals to use their affected hand in a variety of ways to complete ADL in everyday life.

Many stroke survivors attempt to improve their ability to complete ADL by participating in rehabilitation. However, 65% of patients still cannot incorporate the affected hand into their daily activities six months post stroke [16]. In addition, rehabilitation does not always guarantee beneficial results for patients who have more severe stroke-related injuries and motor impairments. Research suggests that rehabilitation is not always the best option for all stroke survivors. Rehabilitation is expensive and limited to clinical environments. These barriers restrict access and force successful recovery to be dependent on the patient's ability to participate in regular sessions and access these care facilities. Rehabilitation must be vigorous, repetitive, systemic and customized for the patient to experience positive results [17]. Some suggest that robotic therapies may be more effective than traditional therapies in certain contexts to support motor function recovery [18]; consequently, researchers have sought out different designs for creating robotic exoskeleton devices that perform robotic therapy and help patients.

There are two types of hand exoskeleton systems currently available: rehabilitative and assistive. Rehabilitative devices are not designed to directly assist individuals in completing ADL. According to [17], the purpose of these rehabilitative devices is to aid the patient in rehabilitation of motor function. They are generally used in a clinical environment with the assistance of a therapist who guides the patient throughout therapy. Purpose-built programs and therapies are incorporated into the device's function. Those programs are performed for a prescribed duration to improve motor function and promote recovery. Rehabilitation devices are typically designed for use in daily living like assistive devices (described below). In this context they present with several limitations, including lack of portability and restricted degrees of freedom (DOFs), limiting overall ADL performance. The reduced DOFs restrain digit motion, therefore limiting the improvement levels of the user's hand dexterity. These types of devices have been tested on patients and researchers found that some survivors showed improvements in functionality, but the subjects were not able to translate said improvement in motor performance to ADL [18]. Stroke survivors cannot directly rely on rehabilitative devices as a method of improving their ability to perform ADL in order to enhance their quality of life.

The second category of exoskeleton devices are assistive devices. They differ from rehabilitative devices in that their purpose is to assist the patient in performing ADL independently or with very little assistance from a clinician. Their portability allows them to be utilized in a variety of settings, including home environments. There are several benefits of assistive devices, including increased accuracy by eliminating user error, affordability and more independent, rigorous and repetitive training. All of these improvements increase the patient's compliance and dedication to rehab. As stated in [18], if devices want to be put into practice, they should reduce the burden of the therapist's job and be low cost. Assistive devices meet that expectation as they are independently operated and listed at affordable prices, especially when compared to rehabilitative devices.

Despite their ability to serve as a better alternative, there are very few assistive devices available. In three separate studies that assessed a variety of devices, less than 32% were assistive in each review [17, 19, 20]. Of those, most were not enough to help patients complete ADL. It is important to remember that ADL requires a variety of hand grasps. Two different studies [21,22] showed that healthy, unimpaired adults use 9 to 11 hand grasps about 80% of the time on a daily basis. Therefore,

we can assume that 9 to 11 hand grasp patterns can achieve 80% of ADL. When excluding the abduction and adduction of the four fingers, the human hand has 17 DOF [Figure 1.1, 23] which are used to perform grasping patterns. This level of dexterity allows all of the joints in each digit to flex and extend to achieve maximum grasping ability. That means at least 17 DOF are required to complete the hand grasps necessary to achieve 80% of ADL. Of the 14 assistive devices reviewed in [19, 20], only 1 of them had 17 DOF. The ability to achieve multiple hand grasp patterns increases the probability of a patient being able to complete ADL. Since most devices are not assistive and those that are assistive cannot complete ADL, we can safely say that there is a dire need for an assistive device that can complete ADL successfully to allow a patient to return to a better quality of life. A hand exoskeleton offering a strategic repertoire of grasp patterns could provide assistive had function, allowing users to use their impaired hand in ways similar to that of an unimpaired limb.

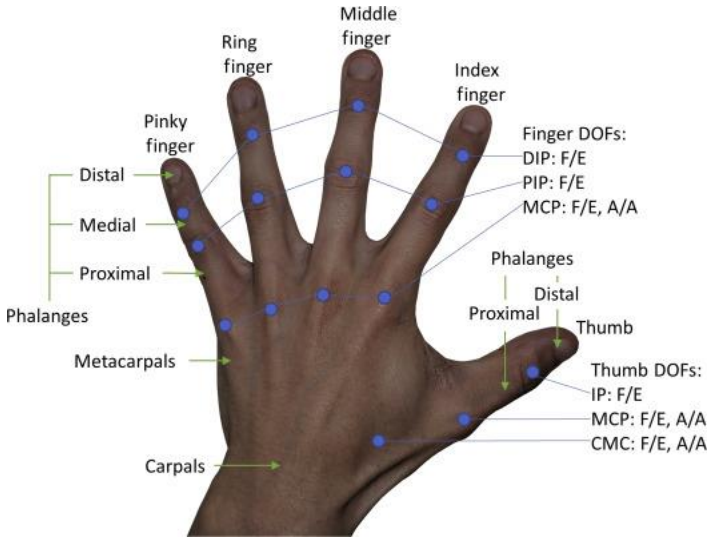

Figure 1.1: Model of Human Hand. Bones are indicated by green lines and joints in blue circles [23]

1.3 Anatomy of the Human Hand

Comprehending the anatomy and physiology of a healthy human hand is necessary to accurately design an effective hand exoskeleton. It helps us understand the biomechanical mechanisms by which stroke-impaired hands may be affected and provides a baseline for the assistive exoskeleton designed in this work.

The movement of the human digits is supported by five major types of structures: bones, ligaments, joints, tendons, and muscles. The bones of the digits provide stability for the hand. Each finger contains distal, middle, and proximal phalanges (Figure 1.2). The thumb is composed of the same bones but does not have a middle phalange. Metacarpal bones are located in the palm of the hand and connect the phalanges to the bones of the wrist. Joints are located in between each phalange and allow movement and rotation of the finger. Each finger has a distal, proximal, and metacarpophalangeal interphalangeal joint (Figure 1.2, Figure 1.3). The thumb has the same joints, except for the distal

interphalangeal joint. The ligaments of the fingers connect each phalange and limit the joint's movement of the finger (Figure 1.3). Collateral ligaments are located on the medial and lateral side of each interphalangeal joint to prevent sideways joint bending. Volar plates are located on the anterior side of each interphalangeal joint and prevent hyperextension.

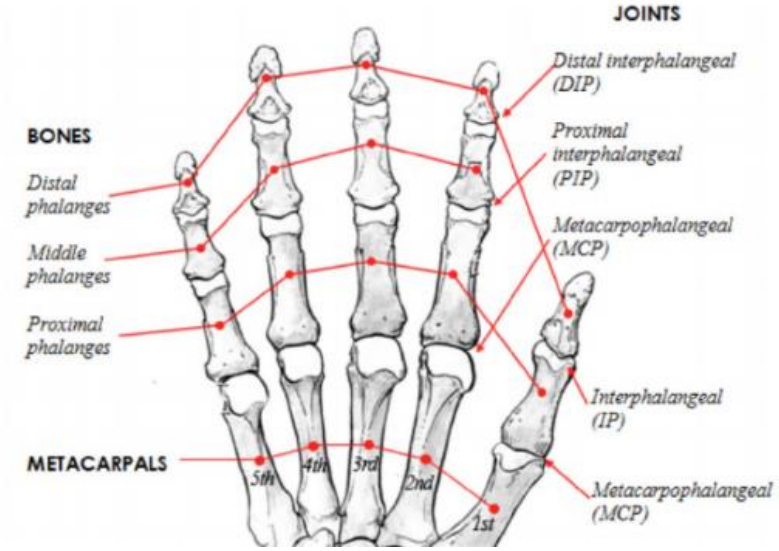

Figure 1.2: Bones and Joints of the Finger and Thumb

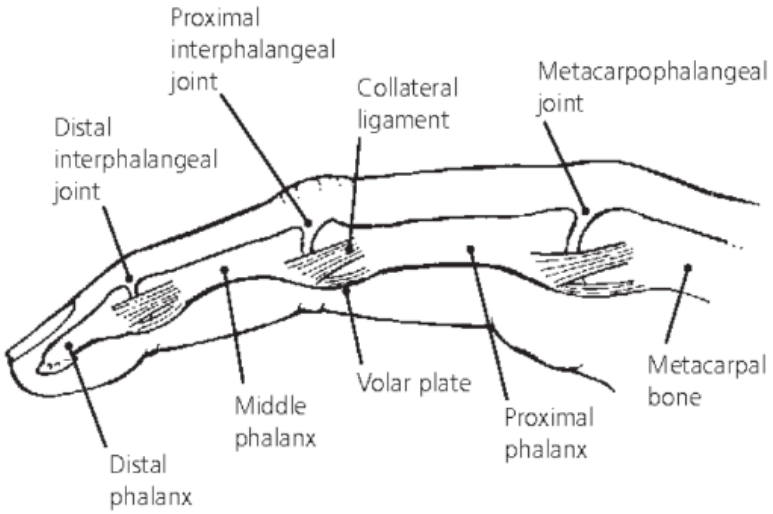

Figure 1.3: Joints and Ligaments of the Finger

The bones of the index, middle and fourth fingers are not proximal to their assigned muscle. They are remotely actuated using long tendons that connect the phalanges to the appropriate muscles in the forearm (Figure 1.4, Figure 1.5). The extensor digitorum muscle on the posterior side of the forearm extends the four fingers via the extensor digitorum tendon. The index finger has an additional extensor tendon called the extensor indicis proprius, which connects to the extensor indicis proprius muscle. The extensor digiti minimi muscle extends the pinky finger via the extensor digiti minimi tendon. The muscles required for the flexion of all fingers are located on the anterior side of the forearm. To flex the fingers, the flexor digitorum profundus and superficialis connect to their respective tendons. The profundus tendon is deep to the superficialis tendon and attaches to the base of the distal phalanx. The flexor digitorum superficialis tendon attaches to the base of the middle phalanx.

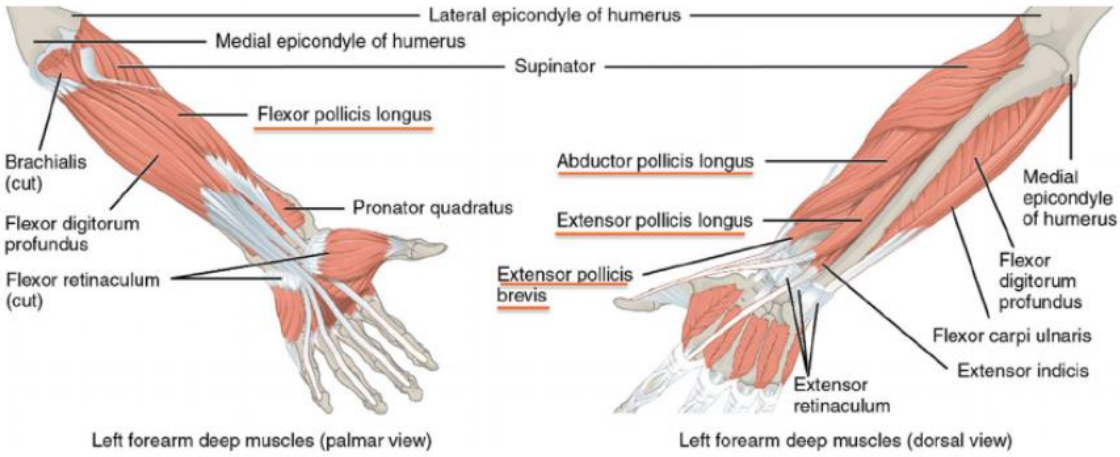

Figure 1.4: Extrinsic Muscles of the Finger

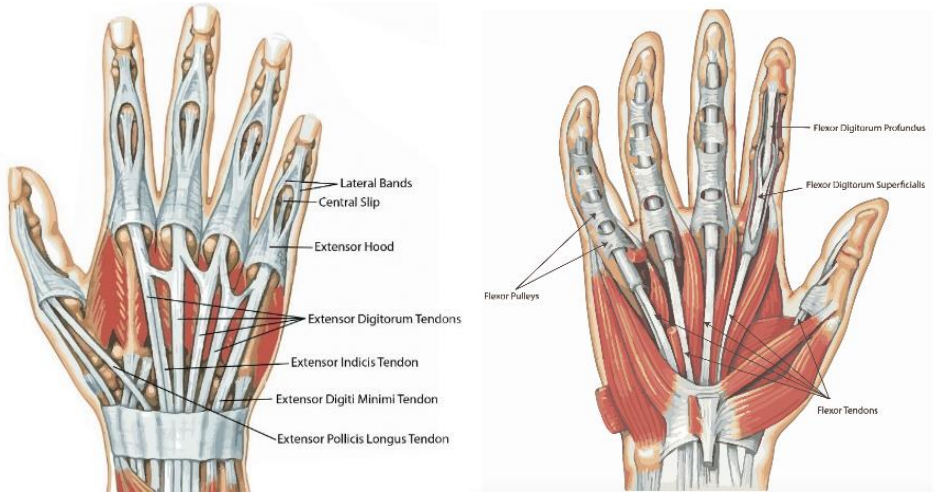

Figure 1.5: Tendons of the Finger and Thumb

The thenar eminence muscle group (Figure 1.6) actuates the thumb and is located on the anterior side of the hand, proximal to the thumb. The adductor pollicis, abductor pollicis brevis, flexor pollicis brevis and opponens pollicis work in tandem give the thumb a wide range of motion. The flexor pollicis longus, abductor pollicis longus, extensor pollicis longus and brevis are located in the forearm and are connected to the bones of the thumb via long tendons for additional flexion and extension.

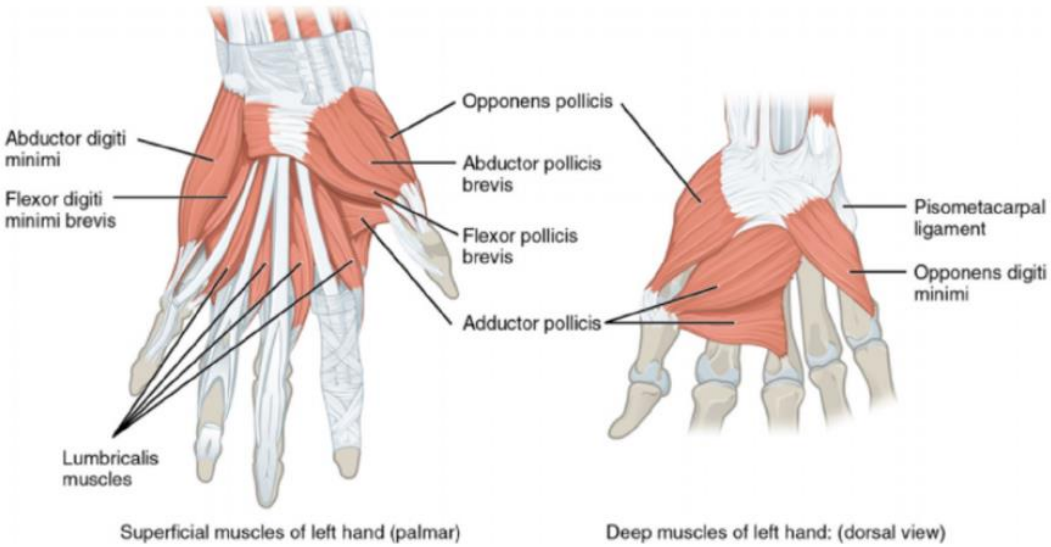

Figure 1.6: Thenar Eminence Muscle Group of the Thumb

When including the abduction and adduction of the four fingers, a healthy human hand has a total of 21 degrees of freedom (DOF) [24] and has the ability to move the digits independently without wrist flexion or extension. However, a hand impacted by stroke, however, often does not have the same mobility, strength and dexterity. A stroke occurs when blood supply to the brain is jeopardized [25]. This is caused by either a blood clot that stops flow to an area of the brain (ischemic stroke) or internal bleeding in the brain due to an artery burst (hemorrhagic stroke). Regardless of the etiology, the resulting damage can cause necrosis or compromise tissue function, much of which supports neural circuits associated with the planning, execution, and find control of movements, resulting in motor impairment [26]. These motor impairments often emerge as spasticity or hemiparesis, as described in the previous chapter. The resulting reduction in dexterity of a stroke survivor's hands leads to a comprised ability to flex and extend the digits. A common method to extend the digits in this case is tenodesis, which involves extension of the wrist and can result in two different grasps: a passive whole hand grip due to digit flexor shortening and a passive lateral grip due to flexor pollicis longus shortening [27]. In summary, able-bodied people can move their digits freely while those impacted by stroke may experience varying levels of difficulty flexing and extending their digits independently.

Of the assistive devices and hand exoskeletons reviewed in [19] and [20], 60% solely focused on flexion. Post stroke, 95% of patients experience spasticity and up to 75% suffer from hemiparesis, meaning

survivors struggle to extend their digits independently [6], a function that is simply not offered by a multitude of hand exoskeleton designs reported in literature. Considering this statistic, it is important to have a device that also encourages the extension of the digits in addition to flexion, a significant gap that many simply do not address.

2 Mechanical Construction of Hand Exoskeleton

This chapter describes the design process of the hand exoskeleton (Figure 2.1). In summary, each digit had a Bowden cable (A) which mechanically linked the left and right portions of the device as depicted in Figure 2.1. Attached to either end of the Bowden cables was nylon string that was used to actuate each digit into flexion or extension. The actuation system (B) on the right side of Figure 2.1 ensured that the string was wrapped around a spool which was stabilized by a spool holder. A servo was affixed to the base of the spool holder to rotate the entire system. As the servo spun, the spool holder and spool rotated, pulling the string and therefore the Bowden cable. The opposite end of the Bowden cable was secured by cable guides hand sewn onto the dorsal side of a glove (C). Nylon string attached to this end of the cable was threaded through the cable guides and anchored to the distal guide. A tension system (D) was included in the design of the hand exoskeleton to allow for tension adjustment in the string to accommodate for different sized hands. The design requirements are listed below in Table 1 and explained in further detail in the sections below.

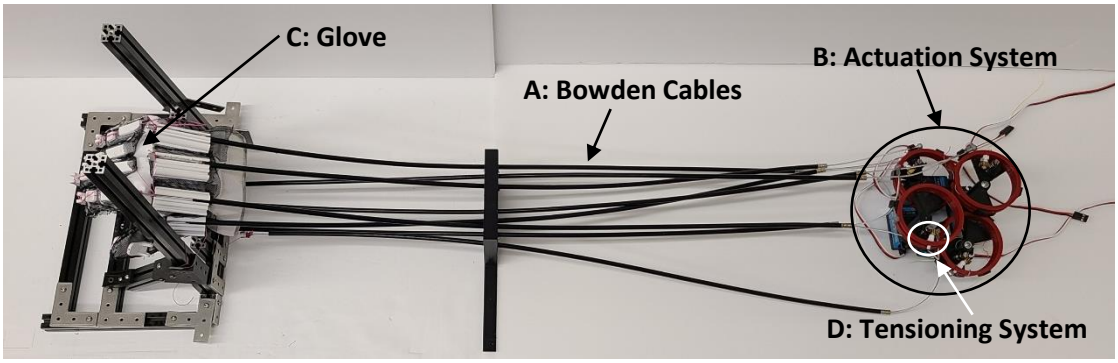

Figure 2.1: Hand Exoskeleton

Design Requirement	Reasoning
Actuation System	
Remote, cable-driven actuation system	Draws inspiration from biological function of human hands
	Reduces complexity
	Allows for a lightweight device
Bowden cable length: 1.92ft	Average distance from human wrist to shoulder, providing adequate space to connect the hand to the actuation system
Minimum servo rotation angle: 180 degrees	150 degrees of rotation was needed to wrap all 5in of nylon string around the spool
	An additional 30 degrees served as an extra margin if needed, totaling to 180 degrees total

Spool radius: 1.91in	Minimum radius for nylon string to wrap around spool with 150 degrees of rotation
	Minimum radius was found using arc length equation
Weight of servo: < 65g	Minimize total weight of actuation system
Minimum torque required of servos: 6.10kg-cm	Minimum torque required to rotate the metacarpophalangeal joint for this design
Glove Design	
Glove made of thin material	Needed to be thin enough to puncture a needle through it for sewing purposes
Material sewn on glove must be porous with minimal flexibility	Holes needed to be large enough to for the first and second layers of filament to adhere to each other during 3D printing
	Minimal flexibility allows the material to stay in place during 3D printing

Table 1: System Design Requirements with Reasonings

2.1 Design of Actuation System

Our design took inspiration from the way healthy human hands drive digits using a system of tendons. The hand exoskeleton used a compact remote actuation system that was fabricated with the intention to be worn on the waist in the future, similar to a waist pouch or fanny pack. This form of remote actuation can be replicated using a hand mounted cable driven system, pneumatics or hydraulics. A cable-driven system was selected since it draws inspiration from the biological function of human hands, reduces complexity, and allows for a lightweight device. Bowden cables have a wire enclosed by a metal casing and rubber sheath to protect the wire from external dangers and allow flexibility. The distance from the wrist to the shoulder provides enough space to connect the hand to the actuation system on the waist. Anthropomorphic tables found in [28] and the average human height of 69.1in [29] were used to determine the that 1.92ft was the appropriate length of the cables. The cables were cut using a Dremel and swage stoppers were secured to the ends of the wires using a press (Figure 2.2).

Figure 2.2: Bowden Cable with Swage Stop

Five inches of nylon string was attached to one end of each cable to eventually connect to a spool, which was rotated using a servo motor. The spool size was dependent on the rotation angle of the servo motors. It was decided that the motors needed to rotate 150 degrees to wrap all 5 inches of the nylon around the spool. An additional 30 degrees was given to serve as an extra margin if needed. Therefore, one of the criteria for the servos was a minimum rotation angle of 180 degrees. Equation 1 was used to determine the radius of the spool. The spool was designed and created in Solidworks (Figure 2.3). Its height was kept at a minimum since the nylon string is extremely thin.

Equation 1

$$arc\ length = 2\pi r\frac{\theta}{360}$$

$$5in = 2\pi r\frac{150}{360}$$

$$r = 1.91in$$

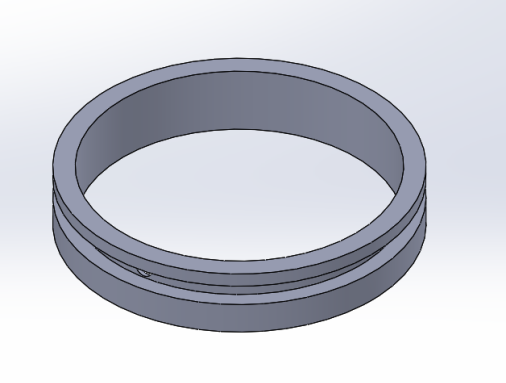

Figure 2.3: Modeled Spool

Spool holders were attached to the spools at the top and anchored to servos on the bottom. The spool holders (Figure 2.4) were at two different heights in an effort to minimize the total space needed to house the actuation system. On the top of the spool holders were wings that hold the spools (Figure 2.5). There were holes at the base of both spool holders that snap onto the output shaft and were secured to the servo using M1.6x4 screws. This allowed the servo to spin the spools indirectly.

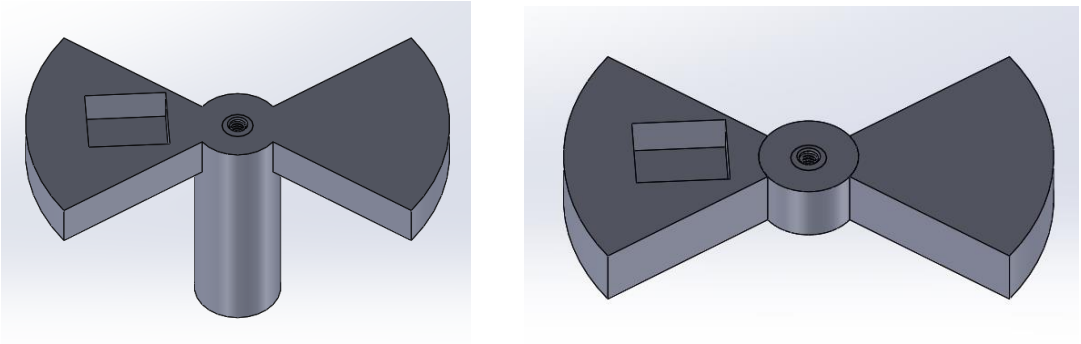

Figure 2.4: Modeled High and Low Spool Holders

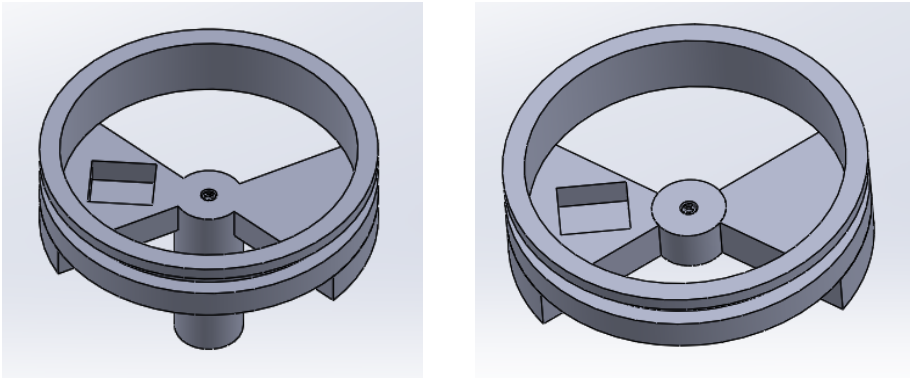

Figure 2.5: Modeled High and Low Spool Holders with Spools Attached

Positional servos were used to actuate the digits of the hand. Several criteria were considered, including minimum rotation angle, weight and torque capabilities. As mentioned previously, the minimum rotation angle for the servos needed to be 180 degrees. The weight of the servo was to be less than 65g. Torque capabilities were determined by understanding the torque requirements of a human hand. Studies analyzing the motor function of post-stroke spastic fingers found that 0.9Nm of torque at the metacarpophalangeal joint is enough to extend the four fingers (excluding the thumb) [30, 31]. An additional 0.025Nm was added as a margin to establish that a minimum value of 0.25Nm of torque per finger should be applied to the metacarpophalangeal joint as determined by [3217]. The distance between the joint and a cable attached on the distal tip of the digit was measured to be 3mm. Equation 2 led to an ideal tension (T) of 8.33N.

Equation 2

$$Tension\ (T) = \frac{Torque\ (\tau)}{d}$$

$$T = \frac{0.25Nm}{0.05m}$$

$$T = 8.33N$$

The required tension considers friction caused by the Bowden cables. According to [33], Equation 3 determines the required tension to account for friction and uses a coefficient of friction of μ = 0.15. The curvature angle was $\frac{5\pi}{6}$ radians, or 150 degrees, as previously mentioned. The required tension, therefore, was found to be 12.34N.

Equation 3

$$T_{req} = Te^{\mu\theta}$$

$$T_{req} = 8.33e^{0.15\left(\frac{5\pi}{6}\right)}$$

$$T_{req} = 12.34N$$

Finally, using Equation 4 the minimum torque required to rotate the metacarpophalangeal joint for this design was 6.10kg-cm. This was the final criteria used to determine the servo used for the actuation system. The servo that met these standards was the ZOSKAY servo motor. Its maximum rotation angle was 270 degrees, allowing for additional rotation if necessary. The maximum torque was 35kg-cm, well above the requirement and weighed 60g.

Equation 4

$$Torque\ (\tau) = F\ x\ d$$

$$\tau = 12.34N\ x\ 1.91in$$

$$\tau = 12.34N\ x\ 0.0485m$$

$$\tau = 0.5986Nm$$

$$\tau = 6.10kg - cm$$

Several designs were considered when deciding on the layout of the actuation housing. After rearranging the servos and modifying the design, a circular layout proved to be the most efficient solution. The actuation system was housed on a circular base with a lid (Figure 2.6). The servos were secured to the base via screws drilled into protrusions attached to the base. They were packed closely together to minimize space. The lid contained two openings for the string and the wires from the servos, allowing easy access to the actuation system. The specifications of the actuation housing are listed in Table 2.

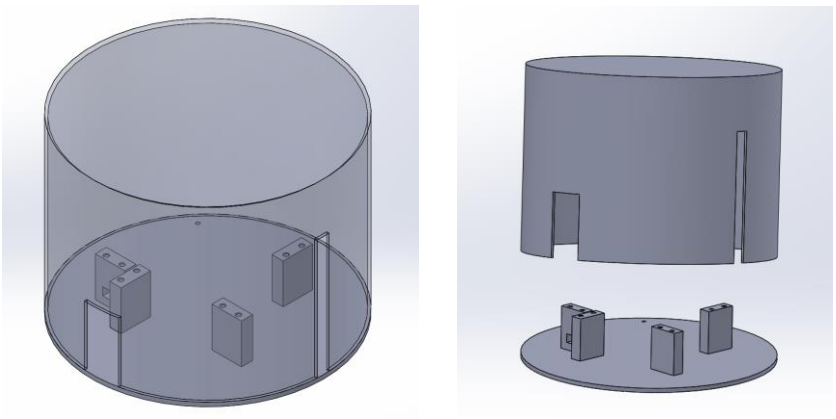

Figure 2.6: Modeled Actuation Housing

Specification	Measurement
Diameter	5.8in
Area	105.58in^2
Surface Area	249.39in^2
Volume	8.96in^3
Mass	0.32lbs

Table 2: Specifications of the Actuation Housing

2.2 Design of the Glove

The glove was to be worn on the hand and contained cable guides to restrict lateral movement of the nylon and Bowden cables. To evaluate our prototype (Chapter 3), a flaccid mannequin hand would later be inserted into this glove to allow it to be actuated and its mechanical electrical performances characterized. The palmar side of the glove contained simple, rectangular guides with holes on either end for the nylon string (Figure 2.7A). They were located perpendicular to the distal, middle and proximal bones. The dorsal side of the glove contained similar guides parallel to the middle and proximal (Figure 2.7B). The dorsal guide parallel to the distal bone on each digit was modeled after the guides found on [32], with modifications including increased thickness and a hole near the bottom for the nylon string (see Figure 2.8 for comparison). The metacarpal cable guide design reported in [3232] were a useful tool to model our design after, but this previous reported design only had one guide for each digit only allowing for digit flexion. Since this exoskeleton was to perform both flexion and extension, there had to be two cables per digit. Therefore, a second slot was added to the metacarpal cable guide and was fitted according to the size of the Bowden cables (see Figure 2.9 for comparison). The length and separation of each guide on both sides of the hand were determined using the measurements from [34].

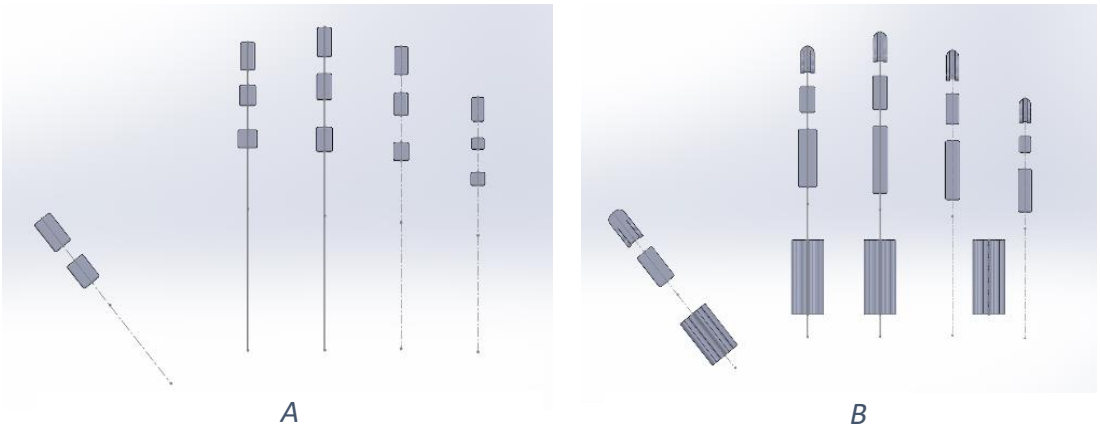

A B

Figure 2.7: Modeled Palmar (A) and Dorsal (B) Guides

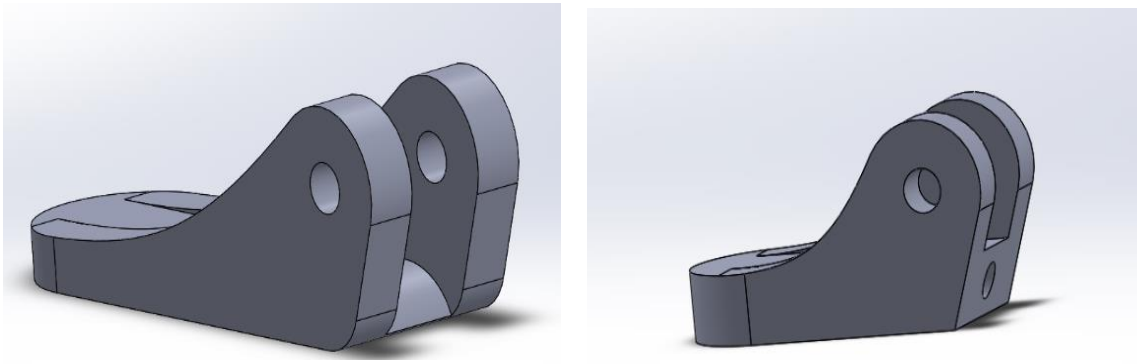

A: Original Distal Cable Guide from [32] *B: Modified Distal Cable Guide*

Figure 2.8: Original (A) vs Modified (B) Distal Cable Guide

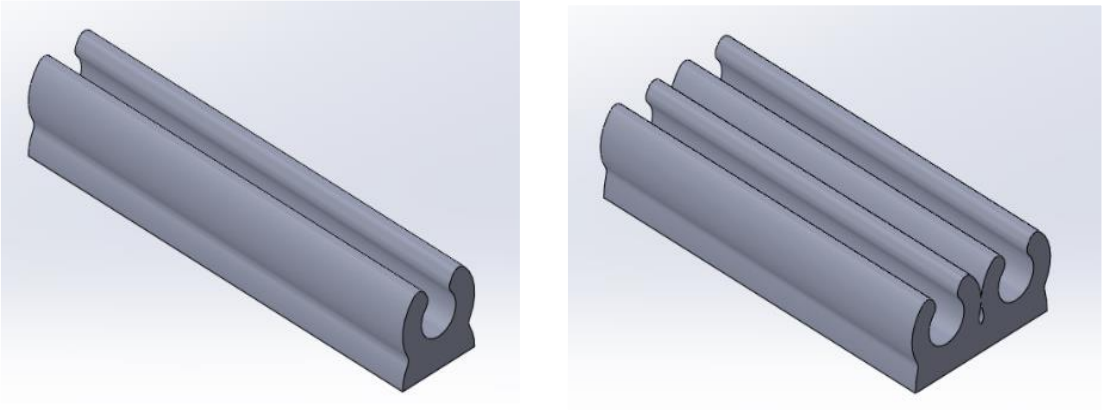

A: Original Metacarpal Cable Guide from [32] B: Modified Metacarpal Cable Guide

Figure 2.9: Original (A) vs Modified (B) Metacarpal Cable Guide

The guides were designed in Solidworks and 3D printed on a mesh material to be attached to the glove. A glove porous enough to 3D print on top of it was not found. It would also not be feasible to print directly on to the glove itself as the filament would penetrate both the dorsal and palmar sides, blocking the digits from entering the desired digit slots on the glove. Nylon mesh spandex, tulle and cotton were deemed viable options to hold the cable guides. They had different sized holes, elasticity and weights. The nylon mesh spandex was favorable since it provided additional elasticity compared to the other two materials. A simple print was tested on each material to determine which would be best. The printing process involved the first filament layer being printed directly onto the print bed of the 3D printer. Once completed, the print was paused, and the fabric material was secured onto the print bed by stretching it taught and using adhesive tape to affix it. The print was then resumed. In theory, the second layer of filament was to attach to the first layer through the material. The cotton material was too thick, and the second layer of filament did not adhere to the first layer. The nylon mesh spandex material was too flexible. The elasticity of the fabric allowed it to move with the nozzle, causing major issues during the print. The tulle material print was successful. It was rigid enough to stay in place during the print. It also had holes large enough for the first and second layers to adhere to each other, but small enough for there to be multiple points of contact between the fabric and filament (Figure 2.10).

Figure 2.10: Dorsal Cable Guides 3D Printed on Tulle Material

The tulle with the guides were hand sewn onto each individual digit of the glove. For this to be possible, the glove needed to be thin enough for a needle to puncture. An athletic football glove, gardening glove and rubber work glove were analyzed to determine which would be best. The gardening glove was too thick, heavy and stiff to be worn comfortably. The rubber work glove was stiff and too small to hold the guides. The athletic football glove had material that was easy to sew onto and provided a snug fit on the mannequin hand (Figure 2.11). It was selected as the appropriate glove for this project.

Figure 2.11: Mannequin Hand Inside the Glove with Cable Guides Sewn onto Glove

2.3 Design of Tensioning System

A unique feature of this hand exoskeleton was the cable tensioning system. This system allowed for an adjustment in the tension of the strings attached to the Bowden cable to accommodate for different sized hands. The string and cables on one side of the hand should be taught when those on the opposite side of the hand are relaxed, similar to the human hand function. The tensioning system started with a guitar tuner, which consists of a handle, worm gear and pinion. The handle was severed from the top of the worm gear, and a notch was created on the top using a Dremel. The notch served as an insert slot for a flathead screwdriver to turn the worm gear. The worm gear was secured to a backing (Figure 2.14) which sits in a slot in the spool holder. The backing was inspired by that of the guitar tuner. The pinion of the guitar tuner remained tangent to the worm gear using a pinion holder (Figure 2.13). It was an original design and was 3D printed. One end held the pinion while the other end was positioned through one side of the spool and had a small hole through which nylon string was threaded. The pinion holder was held perpendicular to the worm gear with a stabilizer (Figure 2.12) and secured onto the spool holder.

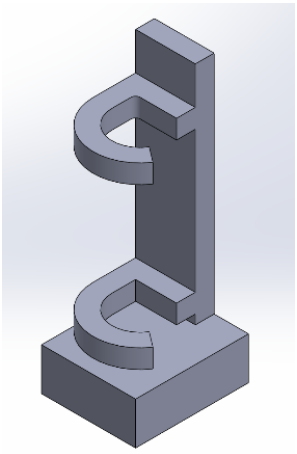

Figure 2.14: Modeled Worm Gear Backing

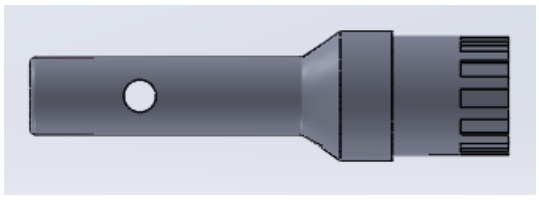

Figure 2.13: Modeled Pinion Holder

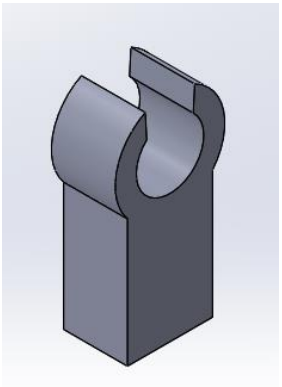

Figure 2.12: Pinion Holder Stabilizer

As a flathead screwdriver turned the worm gear, the pinion gear rotated the pinion holder, allowing the nylon to wrap around it as tension adjustment was needed. The tensioning system (Figure 2.15) sat atop each spool holder. With a mixture of guitar parts and original 3D printed designs, a tensioning system was successfully created.

Figure 2.15: Fully Constructed Tensioning System

A: Worm Gear with notch B: Backing C: Pinion Gear D: Pinion Holder E: Pinion Holder

2.4 Final Design Construction

The majority of the parts used to create the hand exoskeleton were 3D printed. The motors were screwed onto the protrusions of the actuation housing base (Figure 2.16). The protrusions were strategically designed to be in specific locations on the base so the motors could be as close to each other as possible. The location of the protrusions also considered the width of the spools and spool holder wings to avoid collisions when rotating. All spool holders were force fit onto the output shaft of the servos and were secured onto the servos using screws. The tensioning system and spool sat on the wing of the spool holders (Figure 2.17). The lid of the housing was removable and allowed for easy access to the actuation system underneath.

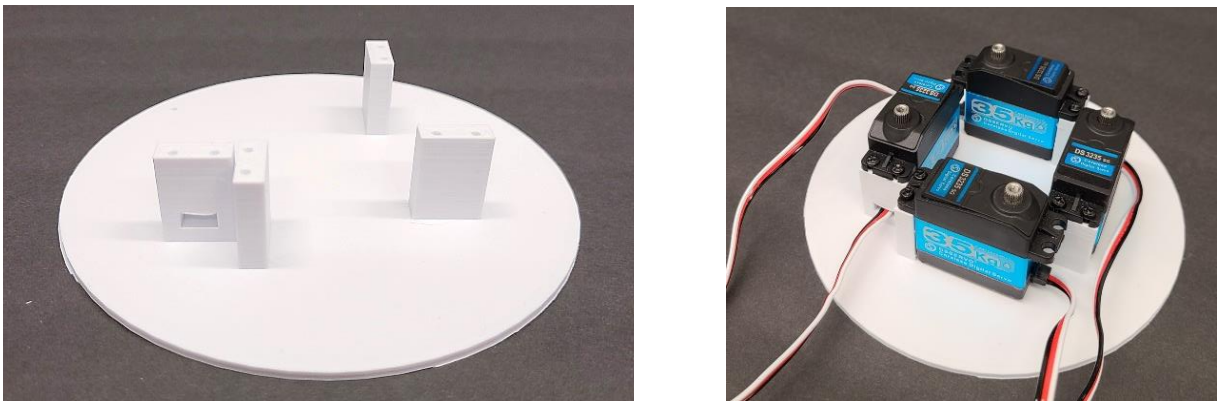

A *B*

Figure 2.16: Actuation Housing Base (A) with Servo Motors Secured (B)

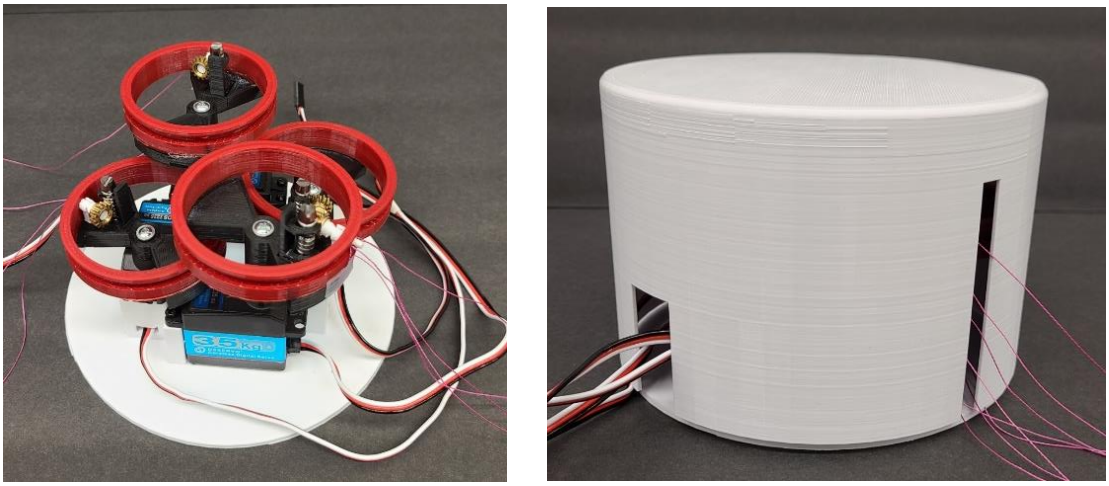

Figure 2.17: Constructed Actuation System and Lid

The Bowden cables connected the glove and hand to the actuation system. Nylon string was secured to each end. One end contained 5 inches of string and was directly attached to the pinion holder as part of the tensioning system. It was also positioned to be wrapped around the spool in order to pull the Bowden cables when the spool rotated. The Bowden cable was kept on the center axis of the spool using a cable holder and bushing (Figure 2.18). On the other end, the Bowden cable was secured using the metacarpal cable guides. The string on this side of the cable was threaded through the holes of the palmar and dorsal cable guides on the glove to flex and extend the digits of the mannequin hand (Figure 2.19).

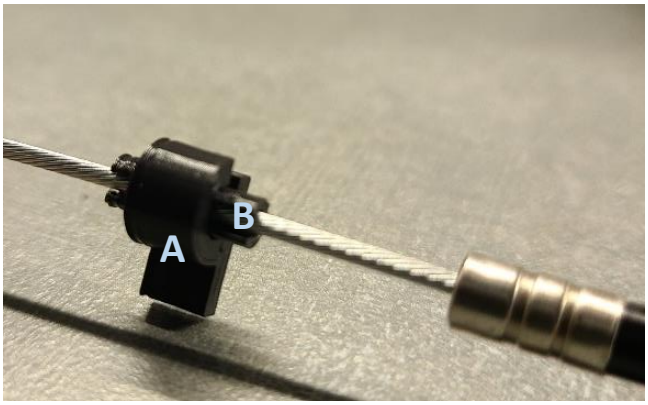

Figure 2.18: Cable Holder (A) and Bushing (B)

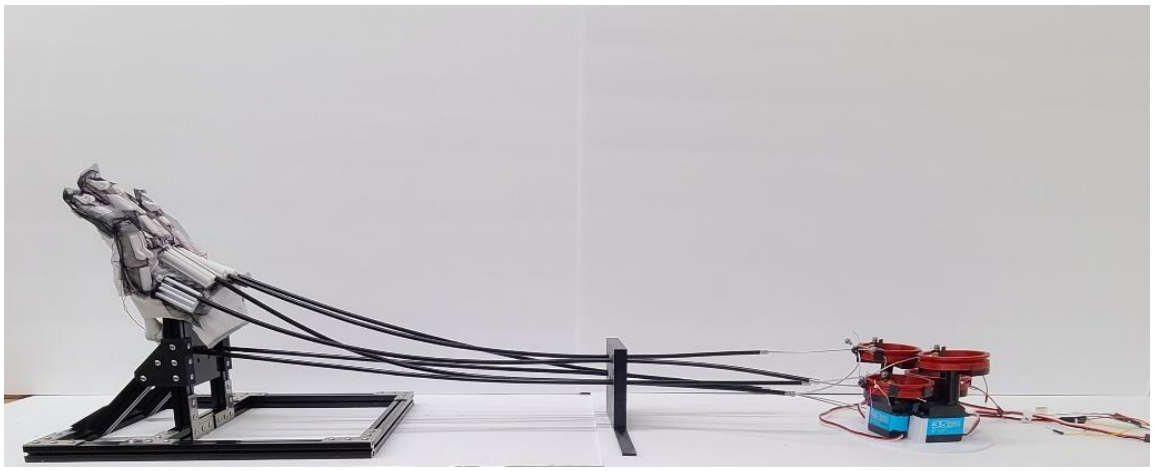

Figure 2.19: Full Mechanical Construction of Hand Exoskeleton

2.5 Control System & Mechanical Construction Integration

An Arduino UNO and breadboard were used to control the hand exoskeleton system. The Arduino UNO was connected directly to the laptop with the software for the code. The breadboard wired the UNO to the servo motors. A diagram showing the wiring is located below in Figure 2.20. The index and middle fingers and thumb were each assigned to a unique servo motor. The fourth and pinky finger shared a servo since in unimpaired hands they typically actuate together in performing ADL. This totaled to four servos powering the digits for flexion and extension. When the digits flexed to complete a hand grasp, the servos rotated the spools counterclockwise. This motion pulled the palmar string and Bowden cables to force the digits on the other end of the Bowden cable to flex. To extend the digits, the servos rotated clockwise to relax the flexion cables and provide tension on the extension string and cables, forcing the digits to extend. This opposing relaxion of the cables and string mimicked the function of the human hand. When the digits are flexed, the flexor muscles contract and the extensor muscles stretch. During extension, the opposite series of actions occur.

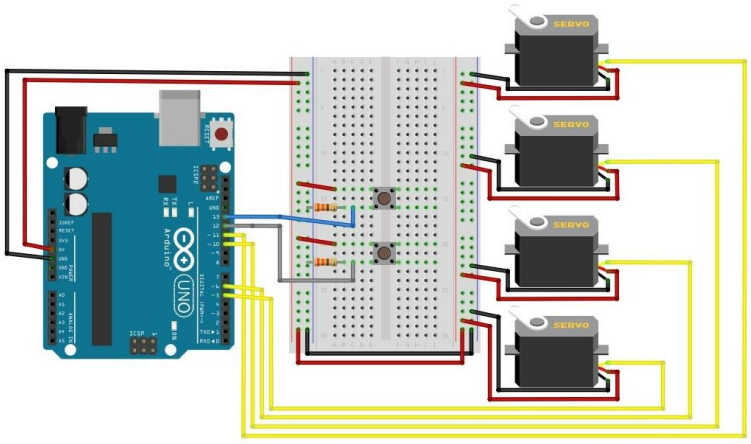

Figure 2.20: Button Wiring Diagram with Servos

3 Experimental Setup & Results

This chapter explains the experimental set up and two different sets of testing. First, the chapter will describe how a low-friction, passive mannequin hand was fabricated and mounted to remain stable during testing such that mechanical and electrical performance of the hand exoskeleton could be evaluated. Next, this chapter illustrates the fabrication of an experimental setup to simultaneously understand the electrical and force characteristics when each digit was actuated. The index finger, middle finger and thumb each went through 10 flexion and 10 extension trials, while the fourth and pinky were actuated together for 10 flexion and 10 extension trials, totaling to 80 trials completed during this first set of testing. Lastly, the second test highlighted in this chapter describes how the wiring was used to direct the mannequin hand to complete various hand grasping movements taken from [35]. Each of these systems and tests are described in further detail in the sections below.

3.1 Design of Mannequin Hand

The goal of this work was to test the mechanical and electrical performance of our design. The presence of a biological hand can introduce a significant amount of resistance, especially for those that may be affected by stroke. Here, the degree of muscle tone and spasticity may be widely varied [36]. For testing, a fully passive hand was required to eliminate the varying degrees resistance that is present in stroke hands and allow for pure mechanical and electrical characterization prior to considering these variables. For this reason, a low-friction passive mannequin hand was deemed necessary to test the performance of the hand exoskeleton. The 21 DOF in healthy hands that we previously described (Section 1.3 Anatomy of the Human Hand) are in the joints of the digit. There are 3 DOF in each finger to flex and extend it and 1 DOF for abduction and adduction. In this design, the extra 1 DOF (abduction and adduction) was not taken into consideration as it does not have a significant impact on the ability to flex and extend the finger. This leaves 12 DOF total needed in the fingers. The human thumb is more flexible and dexterous than the fingers, making it a complicated part of the body. Its complex movements are driven by 5 DOF, all of which need to be accounted for. In total, the mannequin hand needed to have a minimum of 17 DOF in order to closely mimic the human hand and complete common hand grasps.

Hand size was another criterion used to determine the type of mannequin selected. A study [34] measured the palmar side of the hand of 139 male and female total subjects ages. This measurement was taken from the distal tip of the middle finger to the base of the hand. Being that the stroke occurs at similar ratios between men and women, 52% and 48% respectively [3], the joint palmar measurements

were used as a reference guide when selecting a mannequin. The joint lengths of the palm found in [34] ranged from 167.78mm to 220mm. Additional requirements for the mannequin hand included negligible friction or stiffness in the joints and easy replication for future experiments.

Mannequin hands for purchase on various websites did not meet these requirements. Most were wooden replicas and did not have the flexibility to bend. Others, such as nail salon practice hands found online, had the required DOF, but had significant friction in the joints. Purchasing a mannequin hand meeting the criterion proved to be unsuccessful, so 3D printing was considered as an option. A replica of a human hand was found on GrabCad for public download (Figure 3.1, [37]) and was deemed appropriate for this project. The palmar length measured 171.7mm, had all DOF necessary and negligible friction in the joints. The file is saved for reproducibility for future projects.

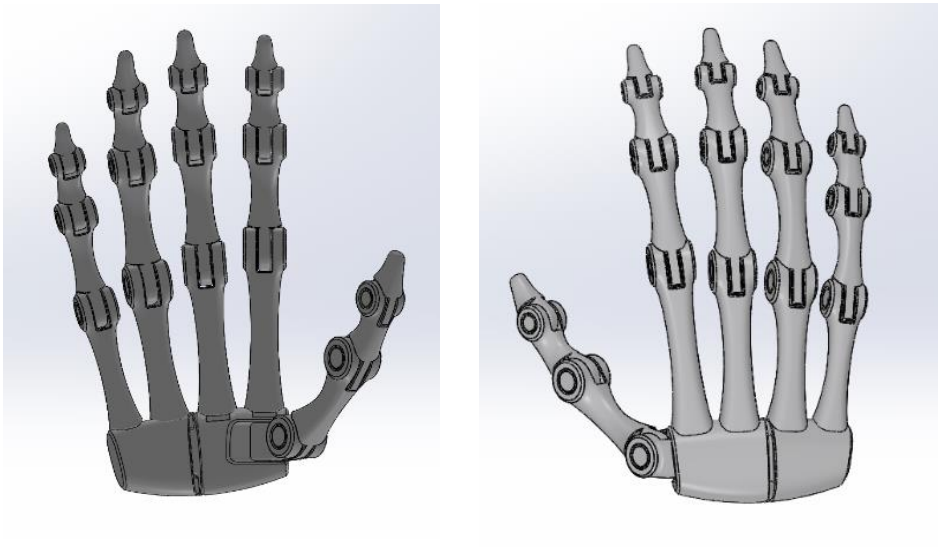

Anterior/Palmar *Posterior/Dorsal*

Figure 3.1: Modeled Mannequin Hand [37]

3.2 Design of Wrist

One of the unique features of the proposed hand exoskeleton is the ability to independently actuate without the assistance of the wrist. That being said, the wrist's sole purpose in this experiment was to mount the hand and hold it upright. A stationary mount (Figure 3.2) was 3D printed using black PLA filament and attached directly to the mannequin hand by screws to hold it vertically in place. The mount was supported by a base made of MakerBeams XL.

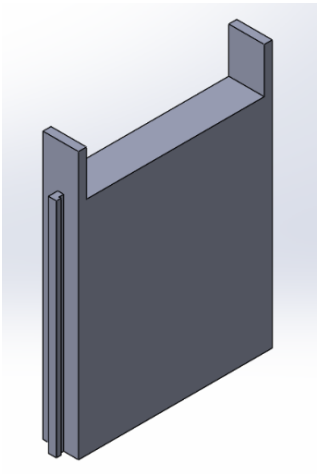

Figure 3.2: Modeled Stationary Mount

3.3 Hand Grasp Selection

One of the main objectives of this project was to design a hand exoskeleton for stroke patients that can complete common hand grasps found in ADL. A study [35] recorded 52 adults performing "real, not simulated, tasks during their normal lives" in order to determine the most common hand grasps of adults. Activities such as eating, drinking, driving and housekeeping were taken into consideration when monitoring hand grasps. To classify the hand grasps, the researchers used 9 grasps from Edwards et al taxonomy [38] that are listed and described in Table 2 and shown in Figure 3.3**Error! Reference source not found.**. This taxonomy was selected because it presented a very complete functional grasps classification and accurately represented the majority of the grasps used in the experiment. The study went on to analyze videos of adults completing a variety of ADL and found how often the nine hand grasps were used in the footage. Over 97% of the footage analyzed included the 9 selected grasps, proving that they were sufficient for the classification of grasps during ADL. This study was used to select the hand grasps to be tested, as this would likely provide future users of the hand exoskeleton with the most functional benefit in ADLs.

Name	Description
Cylindrical grasp (Cyl)	The palm is involved. The thumb is in direct opposition to the fingers (in abduction or neutral)
Oblique palmar grasp (Obl)	Variation of the Cylindrical grasp. The palm is involved, but the thumb is adducted
Hook grasp (Hook)	Palm and thumb are not involved. The object's weight is borne by fingers
Lumbrical grasp (Lum)	Thumb and proximal part of the fingers are involved, but the palm is not involved
Intermediate power-precision grasp (IntPP)	The palm is somewhat involved but both the thumb and index stabilize the grasp
Pinch grasp (Pinch)	Thumb and fingertips (one or more) are used
Lateral Pinch (LatP)	The lateral part of the fingers (one or more) are used, and usually the thumb as well
Special pinch (SpP)	The thumb, lateral part of some finger and the fingertips of another/others are involved
Non-prehensile grasp (NonP)	Objects are manipulated without grasping them

Table 3: Names and Descriptions of Grasps Considered from Taxonomy [35]

Figure 3.3: Examples of Grasps Considered from Taxonomy [35]

3.4 Code & Wiring

A code was created using Arduino for the hand exoskeleton to complete the 9 hand grasps identified in [35]. A command was made specifically for each grasp and listed in Arduino. The code was controlled by two buttons on a bread board. The first button served as a toggle switch so the user could easily and accurately select their desired hand grasp. This was an extremely important feature of the exoskeleton to decrease potential abandonment rates. On average, 50% of prescribed assistive technologies will ultimately be abandoned by stroke survivors [39] and among the largest barriers to these assistive technologies is function and design [40]. A toggle button gives the user full control over the system, reducing the potential for frustration and abandonment. The second button, the actuation button, determines the timing of actuation. When initially pressed, the servos rotate to flex the appropriate digits to complete the desired hand grasp. When pressed a second time, the system rotates in the opposite direction to extend and relax the digits. This allows the digits to flex and extend exclusively at the command of the user. Because Arduino was used, there is open access to the control of the system and provides the benefit of being agnostic to control systems. This allows for future detailed investigations to understand the efficacy of other control systems such electromyography-based systems, or those that used other advanced sensing technologies.

As previously mentioned, the operator could toggle through the common hand grasps using the toggle button and select the desired grasp pattern. Once the actuation button was pressed, the system completed the grasp. For example, the hook grasp was fifth on the list of grasps in the code. To select the hook grasp, the user must press the toggle button five times. Once the user was ready to start the grasp, they would press the actuation button once, and the appropriate servos would rotate in order to flex the necessary digits to complete the desired hand grasp. Individual digit actuation was an additional command added to the list for testing purposes.

3.5 System Characteristics

A calibrated 8mm SingleTact capacitive force sensor with a range of 10N, a Sparkfun ACS723 current sensor and a National Instruments USB-6210 data acquisition system were connected to measure the mechanical and electrical characteristics of each digit (Figure 3.4). A Tekpower, TP-3005D-3 0-30V/0-5A power supply powered the entire system to ensure consistent voltage throughout testing. The force sensor was secured in a 3D printed holder and placed on top of a three-axis adjustable stand made of Maker Beam XLs (Figure 3.5). A MATLAB code was created to measure the current, force and voltage for each trial.

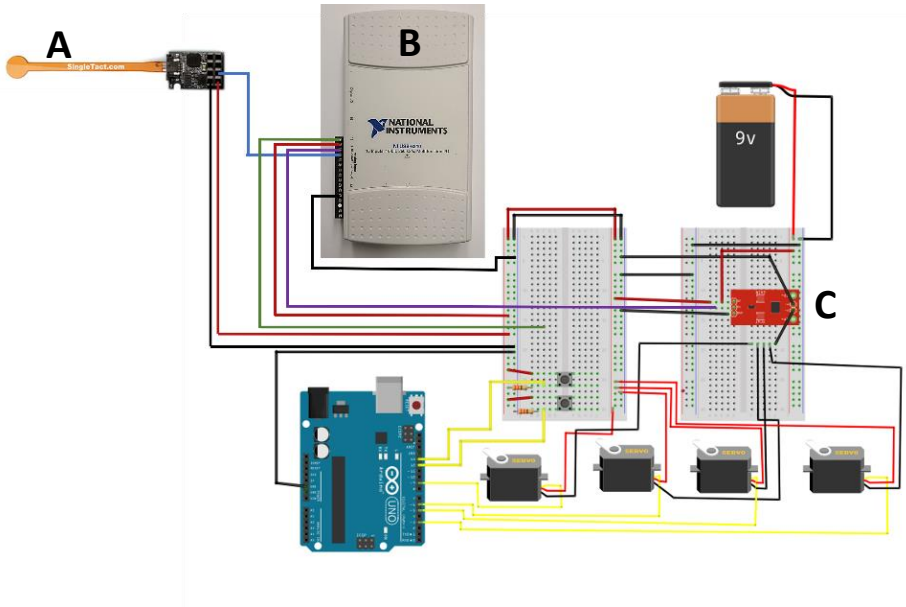

Figure 3.4: Full Wiring Diagram with Force Sensor (A), Data Acquisition System (B) and Current Sensor (C)

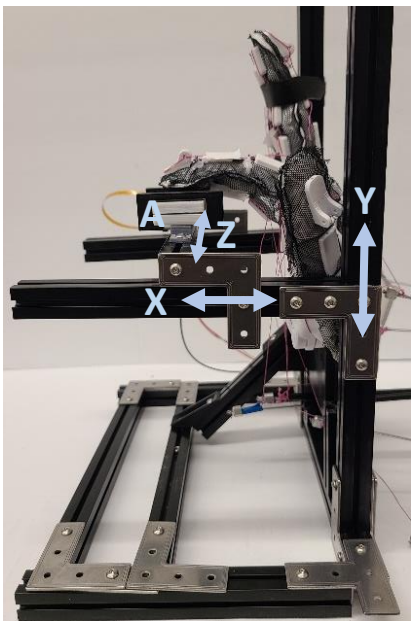

Figure 3.5: Three-Axis (X,Y,Z) Adjustable Stand with Sensor Holder (A)

The first test was conducted to measure and understand the synchronous electrical and mechanical characteristics of each digit when actuated. A MATLAB code was created to collect the prehension force, hand voltage and motor current over the course of 20 seconds and graph these results as sampled at 4000Hz. An example of a resulting graph is labeled in Figure 3.6A. To begin testing, the toggle button on

the controller (described above) was pressed until “Individual Finger Actuation” appeared in the serial monitor of Arduino. The trial was initiated when the MATLAB code was activated. There was a five second gap between the start of the trial and the pressing of the actuation button to capture data before, during and after actuation. It also ensured accurate readings on the graph. For example, an abnormally shaped graph (Figure 3.6B) produced incorrect actuation data and indicated an issue with the force sensor or data acquisition system. During the initial five seconds, the force data collected was minimal and labeled as “C” in Figure 3.6A. Once the five seconds passed, the actuation button was pressed and the assigned servo rotated to pull its Bowden cable to actuate the desired digit towards the sensor holder, applying pressure to the force sensor (Figure 3.7). The digit remained actuated for five seconds. The data collected during actuation is shown in “D” of Figure 3.6A and are the highest points during the trial. Finally, the actuation button was pressed a second time to relax the cable and return the digit back to its original state, removing pressure from the force sensor. As a result, the graph displayed minimal force data similar to the beginning of the trial as shown in “E” of Figure 3.6A. This test was completed for flexion actuation and extension actuation.

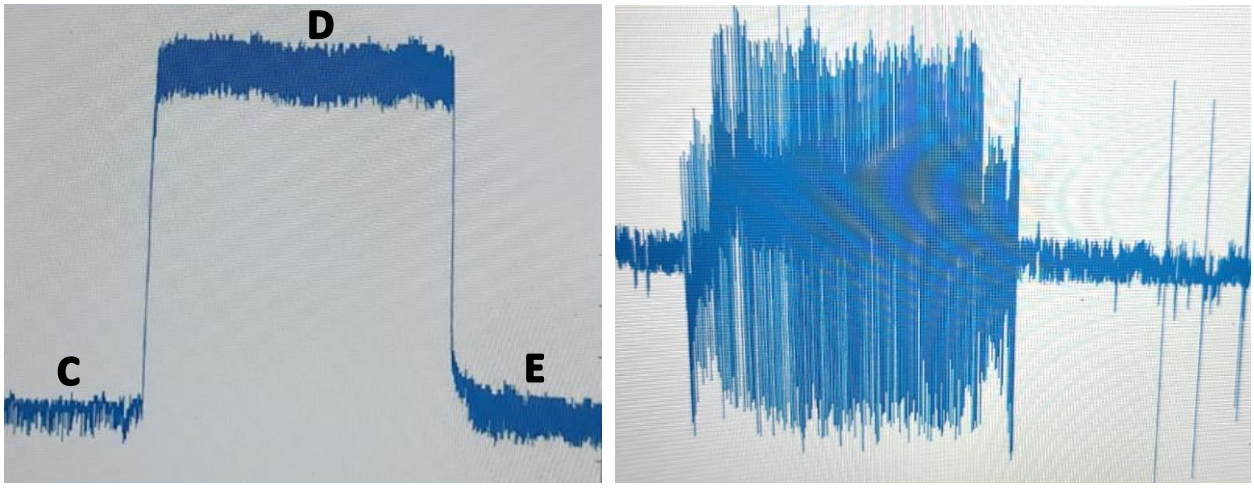

A *B*

Figure 3.6: Example of Correct (A) and Incorrect (B) Force Data Shape Produced by MATLAB

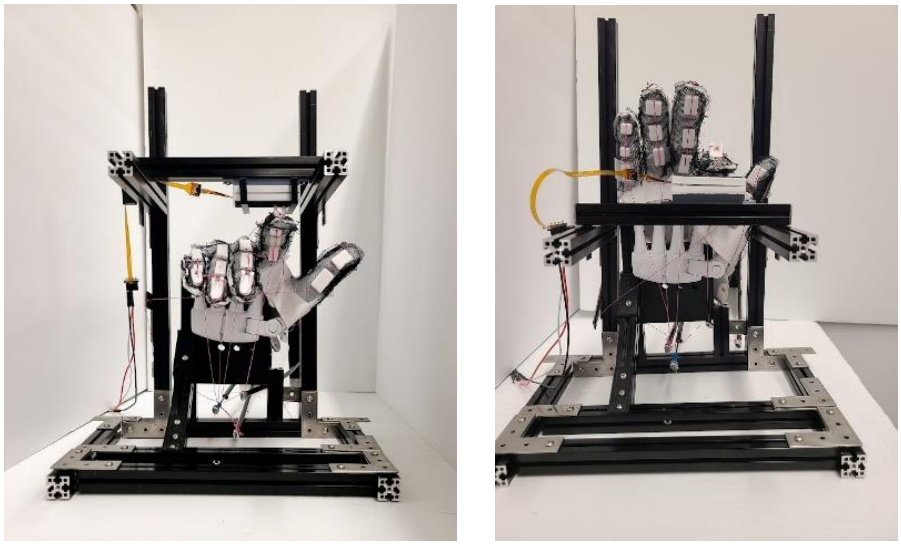

A *B*

Figure 3.7: Digit Extension (A) and Digit Flexion (B) Testing Setups

The next part of this test involved finding the average force, current and power in each of the 80 trials. A second MATLAB code was used to find the 4,000 largest data points of force, current and voltage in a single trial and calibrate them using the calibration curve given with each sensor. This creates a calibrated linear inter-integrated circuit (I2C) output for the sensor's specified input force range of 0N to 10N since the output is determined via MATLAB. These top values represented the data collected only during actuation. The code then used the calibrated 4000 current and voltage values to calculate the power produced during actuation, then found the average force, current, and power of said trial (Table 4, Table 5). The index finger, middle finger and thumb each had 10 flexion and 10 extension trials, while the fourth and pinky were actuated together for 10 flexion and 10 extension trials. The averages for all 80 trials were combined into one data set to compare the average current, force and power produced by each digit (Figure 3.8, Figure 3.9).

	Averages					
	Current (A)	**SD**	**Force (N)**	**SD**	**Power (W)**	**SD**
Index	0.38	0.08	0.69	0.09	1.78	0.34
Middle	0.81	0.30	1.04	0.25	3.12	1.03
Fourth & Pinky	0.12	0.05	0.92	0.12	0.51	0.20
Thumb	1.52	0.05	0.85	0.18	7.42	0.24

Table 4: Average Extension Electrical and Mechanical Characteristics for each Digit (SD = standard deviation)

	Current (A)	Force (N)	Power (W)
Total Averages	0.71	0.88	3.21
SD	0.61	0.15	3.00

Table 5: Average Extension Electrical and Mechanical Characteristics Across All Trials (SD = standard deviation)

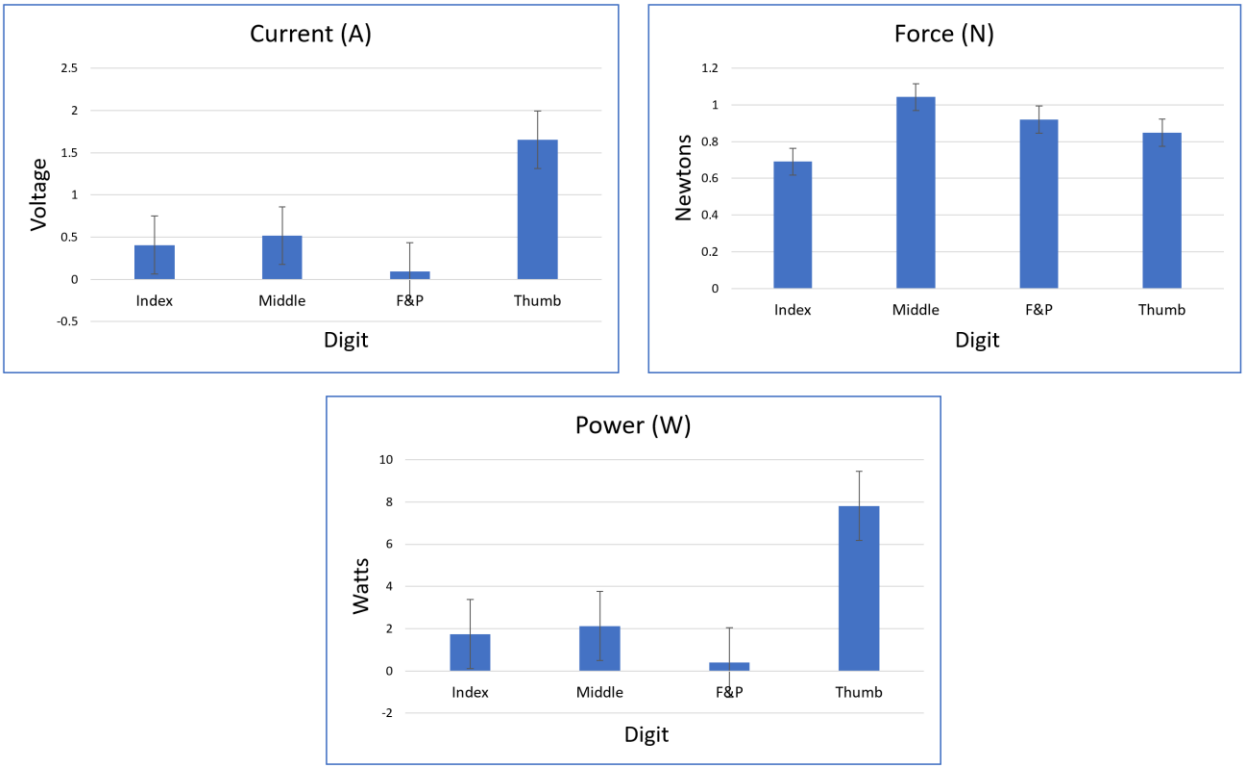

Figure 3.8: Average Current, Force and Power During Extension of Digits with Error Bars

	Averages					
	Current (A)	**SD**	**Force (N)**	**SD**	**Power (W)**	**SD**
Index	0.41	0.05	0.55	0.11	1.74	0.20
Middle	0.52	0.22	0.68	0.18	2.12	0.84
Fourth & Pinky	0.09	0.06	1.07	0.13	0.39	0.25
Thumb	1.65	0.03	1.06	0.11	7.81	0.15

Table 6: Average Flexion Electrical and Mechanical Characteristics for each Digit (SD = standard deviation)

	Current (A)	Force (N)	Power (W)
Total Averages	0.67	0.84	3.01
SD	0.68	0.27	3.28

Table 7: Average Flexion Electrical and Mechanical Characteristics Across All Trials (SD = standard deviation)

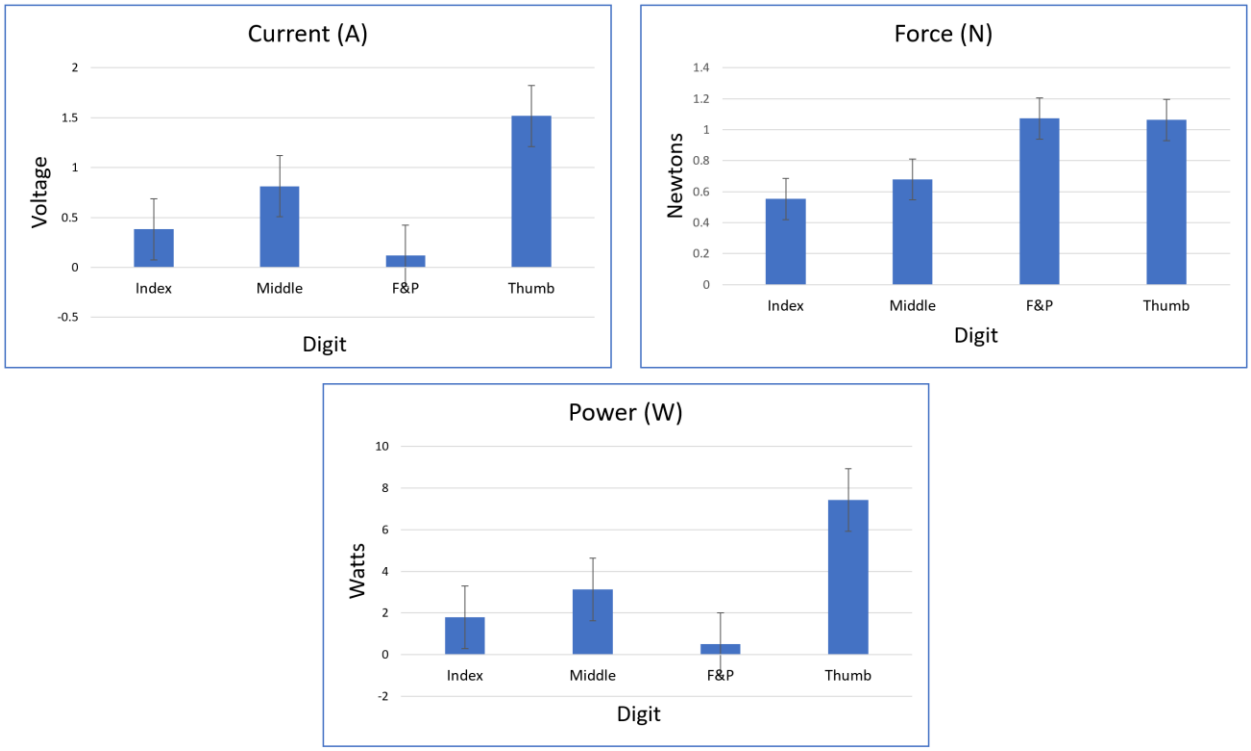

Figure 3.9: Average Current, Force and Power During Flexion of Digits with Error Bars

As mentioned in Chapter 2, the flexor and extensor muscles located in the forearm are responsible for actuating multiple fingers. The hand exoskeleton operates slightly differently, where the servos, representing the muscles, are only responsible for actuating one digit (with the exception of the fourth and pinky fingers). This design simplifies the control system such that there is direct, simple actuation. The values found in this work may not directly correlate to that of the human hand, which is expected due to the difference in design when compared to the human hand.

The measured force outputs for the hand exoskeleton ranged from 0.69N to 1.04N during extension and 0.55N to 1.07N during flexion. The maximum value was from the extension of the middle finger and

flexion of the fourth and pinky fingers. The electrical performance included current and power measurements. For extension, the current and power ranged from 0.38A to 1.51A and 0.51W to 7.42W, where the minimums were found in fourth and pinky finger actuation and thumb actuation, respectively. Similarly, the current and power during flexion ranged from 0.09A to 1.65A and 0.39W to 7.81W, respectively. The minimum and maximum values were in the same digits as extension. Overall, the digits perform fairly similarly during flexion and extension.

3.6 Grasping Capabilities

The hand exoskeleton was designed to complete the 9 common hand grasps described in Section 3.3 Hand Grasp Selection. Using the button system described in Section 3.4 Code & Wiring**Error! Reference source not found.**, the desired grasp was selected prior to pressing the actuation button. Different 3D printed manipulanda were used to test the grasping capabilities of the system (Figure 3.10). A stand was used to stabilize the manipulanda for grasps that did not require thumb flexion.

The manipulanda were designed to incorporate the SingleTact force sensors to measure grasping forces. The same setup as Figure 3.4 was used to collect the data. During testing, the data acquisition system and force sensors often produced noisy and inaccurate data. Both the sensor and wires were replaced in an attempt collect clean data, but it remained unusable. Multiple significant integration, hardware and software issues emerged that made collecting detailed grasping data with the manipulanda beyond ethe feasible timelines and scopes of this master's thesis. Therefore, the manipulanda was solely used to demonstrate the hand exoskeleton's ability to complete common hand grasps.

Figure 3.10: Hand Exoskeleton Performing Common Hand Grasps using Manipulanda

3.7 Grasping Characteristics

While the technical challenges prevented the collection of grasping characteristics when multiple digits actuated in coordination to grasp manipulanda, the data of the individual digits could be used to estimate the results. After analyzing the grasps, the specific digits actuated for each grasp were determined in order to calculate the estimated mechanical and electrical outputs of the grasps. Table 8

describes which digits are actuated in each grasp. It's important to recall that the index finger, middle finger and thumb are each powered by one servo, while the fourth and pinky fingers are powered simultaneously by one servo, totaling to 4 total servos when all the digits are actuated. To estimate the current draw for each hand grasp, the average flexion current of the actuated digits found in Table 4 was added together (see example Equation 5). The same calculation was completed for the estimated force and power produced for each grasp. For example, the pinch grasp required the actuation of the index finger and thumb. To find the estimated mechanical output, the average force of the index finger and thumb were added together. Below, Table 8 presents the assumed electrical and mechanical outputs for the eight grasps that require flexion.

Equation 5

$$Estimated\ Pinch\ Current\ Draw = Index\ Flexion\ Current\ Draw + Thumb\ Flexion\ Current\ Draw$$

$$Estimated\ Pinch\ Current\ Draw = 0.41A + 1.65A$$

$$Estimated\ Pinch\ Current\ Draw = 2.06A$$

	Fingers Actuated				**Estimated Electrical and Mechanical Output**		
Grasp	Index	Middle	Fourth & Pinky	Thumb	Estimated Current Draw (A)	Estimated Force Produced (N)	Estimated Power Draw (W)
Cylindrical	x	x	x	x	2.67	3.37	12.06
Oblique Palmar	x	x	x		1.02	2.30	4.25
Hook	x	x	x		1.02	2.30	4.25
Lumbrical	x	x	x	x	2.67	3.37	12.06
Intermediate Power-Precision	x			x	2.06	1.62	9.55
Pinch	x			x	2.06	1.62	9.55
Lateral Pinch				x	1.65	1.06	7.81
Special Pinch	x	x		x	2.58	2.29	11.67

Table 8: Estimated Electrical and Mechanical Output of Grasps

4 Conclusion & Future Work

4.1 Conclusion

While there are several robotic devices that focus on motor function recovery, none are assistive devices specifically designed to perform common hand grasps in order to complete ADL. This type of device may provide opportunities to allow a patient to return to independence and an improved quality of life. Here, a hand exoskeleton for hand-impaired patients was designed specifically to execute 9 common hand grasps found in adults to complete ADL and achieve both flexion and extension. This unique device was created using low-cost and easily accessible material to promote its accessibility. The mechanical and electrical traits were found in order to characterize the device's performance.

During the testing of the system, there were several limitations. During ADLs, most grasp types are applied to objects that are lighter than 500g (4.9N) [41], but the output forces of our devices do not reach this value. This limits our ability to test the exoskeleton's grasping capability using real-world objects. Other designs described in literature used healthy subjects and are able to produce 15N of grip force [42, 43], successfully grasp a 1L plastic water bottle (a ~1000g load) [44], or use EMG signals to detect the intent of the wearer [45].

There were several accomplishments within this work. We built a hand exoskeleton that can successfully complete common hand grasps found in adults and determined the electrical and mechanical characteristics of the system. In addition, 80% of the parts are 3D printed, making the exoskeleton inexpensive, reproduceable and customizable. However, there were challenges that were faced during the performance characterization of the system. The data acquisition system and force sensors often produced noisy and inaccurate data during testing. We also found multiple servo motors to be defective which made consistent actuation of digits a challenge with replacement of these motors occurring frequently. This resulted in numerous trials being required to collect 10 clean data sets for each digit. Finally, there were challenges with the tensioning system. It proved to be more effective for the cables to also wrap around the spool during servo rotation instead of only the nylon string. This approach provided enough force to pull the digit in the desired direction. In future iteration of this design, we'd suggest creating a 3D printed structure to stabilize the Bowden cables and keep them on the same horizontal plane as their assigned spools. Designing a spool that includes a partial enclosure would also keep the nylon string and cable on said horizontal plane. Lastly, shortening the metacarpal cable guides and incorporating the tensioning system between the proximal and metacarpal cable guides could make the tensioning system more successful.

During testing, the electrical characteristics of current and power were tabulated to provide a baseline of electrical performance. It was found during testing that the lowest and highest current draw, power draw and force were recorded during flexion. The lowest average current and power draw were 0.092A and 0.393W, respectively. These results corresponded to the actuation of the fourth and pinky fingers which was anticipated as a single digit was being activated and with minimal frictional forces present. These values are expected as a single servo took on the task of actuating two digits. The values for the maximum current and power draw were 1.65A and 7.42W which were both recorded during thumb actuation. The index finger was responsible for the minimum force of 0.55N, while the maximum force of 1.07N was from the fourth and pinky fingers. It is good to note that the difference between the index and middle finger's flexion force measurements was less than 0.15N. Therefore, these force values are anticipated since a single servo takes on only one digit, while another servo is responsible for the

actuation of two digits. Overall, these values provide the necessary information to allow for future untethered battery-operated control.

4.2 Future Work

There are several improvements that can be made to the hand exoskeleton in its current state. The calculations to determine the mechanical and electrical characteristics of each grasp were determined by adding together the digits of the individual digits actuated in said grasp. This approach was taken as numerous bugs in the control and data collection system prevented the direct measurement of these values. As previously mentioned, the force sensors and data acquisition system repeatedly generated inconsistent and unusable data. Numerous attempts were made to debug the code, and we rewired the system to ensure clean conduction and communication. Even still, extremely noisy data remained an issue. We believe a new data acquisition system or force sensor is needed to determine the true cause of the inconsistent data. The tested mechanical and electrical characteristics of each grasp can then be found using the control system.

In the future, we would also like to continue to decrease the size of the actuation housing. This would require utilizing smaller, reliable servos and designing smaller spools. Currently, the mannequin hand returns to its original state via gravity. To further improve our work, the system should be adjusted such that the digits are returned to their resting positions using actuation. Next, we would like to conduct the anthropomorphic hand assent protocol (AHAP) test using a stronger mannequin hand [46]. The AHAP test will allow for the exoskeleton's grasping and maintaining ability to be evaluated when manipulating common household objects and benchmarked against other assistive devices. The objective of performing the comparisons will be to validate the system’s performance and viability as a research platform. Post AHAP testing, the exoskeleton can be adjusted accordingly to be suitable for patient testing. During this phase, the goal would be to test the hand exoskeleton on patients with varying levels of dexterity disabilities and determine the electrical and mechanical characteristics, as well as its ability to perform grasps with impaired patients. As mentioned previously, the actuation system would be reduced in size to be worn on the waist, similar to a waist pouch or fanny pack. The Bowden cables would run on the posterior and anterior sides of the forearm and connect to the glove that would be worn on the affected hand.

4.3 Future Suggestions

Should anyone undertake this research, there are suggestions from the authors that can enhance the hand exoskeleton and the testing experience.

As mentioned in Chapter 2.2 Design of the Glove, the characteristics of the material on which the cables guides are printed is imperative. If future researchers decide to use a different material, they need to make sure it is a porous, fairly rigid material. While a stretchy, elastic material would theoretically allow for additional flexibility for the user wearing the glove, it is not conducive to use for 3D printing because it moves with the nozzle of the extruder. This will likely cause major 3D printer issues that could lead to a failed print or breaking the printer. When 3D printing with the chosen material, use something to secure it to the bed plate of the printer. Large paper clips were used to anchor the tulle material used in this research. During the beginning of the print, it may also be helpful to physically hold the material

down on the print bed for additional support. It's recommended to watch the first 3-5 layers to make sure they adhere correctly through the material.

If another mannequin hand is used to test the exoskeleton, it is imperative for it to have negligible friction in the joints of each digit. Otherwise, friction characteristics will need to be measured during the experimentation and testing phase. The hand used in this work was prepared on BCN3D Stratos software and printed on a Sigmax R19 BCN 3D printer. It's advised that the infill settings are changed to 30% instead of 20%, especially if using a similar printer. After the mannequin hand finishes printing, a small force must be applied to each joint of the digits to break the supports and allow for smooth rotation. Without the proper infill, the filament will not be strong enough to withstand the force, causing parts of the phalange to snap off. This print can be time consuming and breaking it can cause delays in experimentation.

To ensure proper flexion and extension of each digit, create a device to hold the Bowden cables near the same vertical axis as their assigned spools. This will allow for better actuation of the digit and reduces the impact of gravity on the overall system. It also keeps the cables steady as the spools rotate and pull on the cables.

A three-axis adjustable stand mentioned in Chapter 3.5 System Characteristics (Figure 3.5) for the force sensor holder increased the efficiency of the system. Rather than rebuilding the whole stand to accommodate the testing the flexion and extension characteristics of each individual digit, the MakerBeams associated with the sensor holder were quickly readjusted to a useful position to ensure accurate data collection. It's suggested this remains for future experimentation.

The servos used in this work were ZOSKAY 35kg high torque coreless motor servos. The authors recommend avoiding these servo motors as they were unreliable and inconsistent. To ensure efficient and accurate testing, find higher quality servo motors that are dependable.

Lastly, the coding portion of the testing design can be adjusted for more efficient data collection. The MATLAB code described in Chapter 3.5 System Characteristics ran one trial at a time and chronologically organized the data in an Excel document. The collect enough data, the code was manually initiated 10 times to get 10 sets of data for one digit. Because each digit completed flexion and extension, the authors initiated over 100 total trials manually and analyzed 100 Excel spreadsheets over the course of experimentation. Instead, the authors suggest writing a code that loops through the trial sequence 10 times when initiated once, with a recommended 5-7 second gap in between each sequence. In this case, the data of 10 trials for one digit can be collected with one manual initiation of the code and stored in one Excel spreadsheet. This produces a more efficient testing process and keeps all of the data for each digit in one location. It will also reduce analysis time. If reliable servo motors are used, creating a loop in Arduino that mimics the timing of the code in MATLAB for each digit would also reduce experimentation time.

4.4 Acknowledgements

The authors would like to thank Marcus Battraw and Peyton Young for their assistance in this work. Special thanks to Kevin and Etiennette Harris, Annie Jones, Terence I. Thurman, Chanise Taylor, Donovan Dooley, Leonard "Top" Robinson, Warren Semien and DuPage AME Church Sunday School for their unwavering support throughout this research.

References

1. Centers for Disease Control and Prevention. (2021, May 25). *Stroke facts*. Centers for Disease Control and Prevention. Retrieved March 23, 2022
2. Global Burden of Disease. (n.d.). *Frequently asked questions*. Institute for Health Metrics and Evaluation. Retrieved October 18, 2022, from https://www.healthdata.org/gbd/faq#Top
3. World Stroke Organization. (2019). *Global Stroke Fact Sheet 2019* [Fact sheet].
4. Mawase, F., Cherry-Allen, K., Xu, J., Anaya, M., Uehara, S., & Celnik, P. (2020). Pushing the Rehabilitation Boundaries: Hand Motor Impairment Can Be Reduced in Chronic Stroke. Neurorehabilitation and Neural Repair, 34(8), 733–745. https://doi.org/10.1177/1545968320939563
5. Pollock, A., Baer, G., Campbell, P., Choo, P. L., Forster, A., Morris, J., Pomeroy, V. M., & Langhorne, P. (2014). Physical Rehabilitation Approaches for the recovery of function and mobility following stroke. *Cochrane Database of Systematic Reviews*, *2014*(4). https://doi.org/10.1002/14651858.cd001920.pub3
6. Schinwelski, M. J., Sitek, E. J., Wąż, P., & Sławek, J. W. (2019). Prevalence and predictors of post-stroke spasticity and its impact on daily living and quality of life.
7. Jin, Y., & Zhao, Y. (2018). Post-stroke Upper Limb Spasticity Incidence for Different Cerebral Infarction Site. *Open medicine (Warsaw, Poland)*, *13*, 227–231. https://doi.org/10.1515/med-2018-0035
8. American Heart Association. (2019, April 8). *Hemiparesis*. www.stroke.org. Retrieved August 21, 2022 *Neurologia i Neurochirurgia Polska, 53*(6), 449. http://dx.doi.org/10.5603/PJNNS.a2019.0067
9. Uswatte, G., Taub, E., Lum, P., Brennan, D., Barman, J., Bowman, M. H., Taylor, A., McKay, S., Sloman, S. B., Morris, D. M., & Mark, V. W. (2021). Tele-rehabilitation of upper-extremity hemiparesis after stroke: Proof-of-concept randomized controlled trial of in-home constraint-induced movement therapy. *Restorative Neurology and Neuroscience*, *39*(4), 303–318. https://doi.org/10.3233/rnn-201100
10. Northwell Health. (n.d.). *Hemiparesis*. Hemiparesis - Institute for Neurology and Neurosurgery | Northwell Health. Retrieved March 23, 2022, from https://www.northwell.edu/neurosciences/conditions/hemiparesis
11. Roby-Brami, A., Jarrassé, N., & Parry, R. (2021). Impairment and compensation in dexterous upper-limb function after stroke. from the direct consequences of pyramidal tract lesions to behavioral involvement of both upper-limbs in daily activities. *Frontiers in Human Neuroscience*, *15*. https://doi.org/10.3389/fnhum.2021.662006
12. Li, S., Latash, M. L., Yue, G. H., Siemionow, V., & Sahgal, V. (2003). The effects of stroke and age on finger interaction in multi-finger force production tasks. *Clinical Neurophysiology*, *114*(9), 1646–1655. https://doi.org/10.1016/s1388-2457(03)00164-0
13. Edemekong, P. F., Bomgaars, D. L., Sukumaran, S., & Levy, S. B. (2022). *Activities of Daily Living*. StatPearls Publishing.
14. Katan, M., & Luft, A. (2018). Global burden of stroke. *Seminars in Neurology*, *38*(02), 208–211. https://doi.org/10.1055/s-0038-1649503
15. Hunter, S., & Crome, P. (2002). Hand function and stroke. *Reviews in Clinical Gerontology, 12*(1), 68-81. doi:10.1017/S0959259802012194
16. Dobkin B. H. (2005). Clinical practice. Rehabilitation after stroke. The New England journal of medicine, 352(16), 1677–1684. https://doi.org/10.1056/NEJMcp043511
17. Khalid, S., Alnajjar, F., Gochoo, M., Renawi, A., & Shimoda, S. (2021). Robotic assistive and rehabilitation devices leading to motor recovery in upper limb: a systematic review. *Disability*

and Rehabilitation: Assistive Technology. https://doi.org/doi.org/10.1080/17483107.2021.1906960
18. Chang, W. H., & Kim, Y. H. (2013). Robot-assisted Therapy in Stroke Rehabilitation. *Journal of stroke*, *15*(3), 174–181. https://doi.org/10.5853/jos.2013.15.3.174
19. Shahid, T., Gouwanda, D., Nurzaman, S. G., & Gopalia, A. A. (2018). Moving toward Soft Robotics: A Decade Review of the Design of Hand Exoskeletons. *Biomimetics* , *3*(17). https://doi.org/10.3390/biomimetics3030017
20. Ferguson, P. W., Shen, Y., & Rosen, J. (2020). Hand exoskeleton systems—overview. *Wearable Robotics*, 149–175. https://doi.org/10.1016/b978-0-12-814659-0.00008-4
21. Bullock, I. M., Zheng, J. Z., De La Rosa, S., Guertler, C., & Dollar, A. M. (2013). Grasp frequency and usage in daily household and machine shop tasks. *IEEE Transactions on Haptics*, *6*(3), 296–308. https://doi.org/10.1109/toh.2013.6
22. Zheng, J. Z., De La Rosa, S., & Dollar, A. M. (2011). An investigation of grasp type and frequency in daily household and machine shop tasks. *2011 IEEE International Conference on Robotics and Automation*. https://doi.org/10.1109/icra.2011.5980366
23. Ferguson, P. W., Shen, Y., & Rosen, J. (2020). Hand exoskeleton systems—overview. *Wearable Robotics*, 149–175. https://doi.org/10.1016/b978-0-12-814659-0.00008-4
24. ElKoura, G., & Singh, K. (2003). Handrix: Animating the Human Hand. *Eurographics/SIGGRAPH Symposium on Computer Animation.*
25. Denslow, E. (2018, January 18). 9 Major Areas of the Brain Affected by Stroke: How Location Impacts Effects & Recovery [web log]. Retrieved August 15, 2022.
26. Hatem, S. M., Saussez, G., della Faille, M., Prist, V., Zhang, X., Dispa, D., & Bleyenheuft, Y. (2016). Rehabilitation of motor function after stroke: A multiple systematic review focused on techniques to stimulate upper extremity recovery. *Frontiers in Human Neuroscience*, *10*. https://doi.org/10.3389/fnhum.2016.00442
27. Mateo, S., Revol, P., Fourtassi, M., Rossetti, Y., Collet, C., & Rode, G. (2012). Kinematic characteristics of tenodesis grasp in C6 quadriplegia. *Spinal Cord*, *51*(2), 144–149. https://doi.org/10.1038/sc.2012.101
28. Winter, D. A. (2009). *Biomechanics and motor control of human movement* (4th ed.). John Wiley & Sons, Inc.
29. Marcin, A. (2022, March 4). *How tall is the average man?* Healthline. Retrieved September 1, 2022, from https://www.healthline.com/health/average-height-for-men#u-s-height
30. Kamper, D. G., & Rymer, W. Z. (2000). Quantitative features of the stretch response of extrinsic finger muscles in hemiparetic stroke. *Muscle & Nerve*, *23*(6), 954–961. https://doi.org/10.1002/(sici)1097-4598(200006)23:6<954::aid-mus17>3.0.co;2-0
31. Kamper, D. G., Fischer, H. C., Cruz, E. G., & Rymer, W. Z. (2006). Weakness is the primary contributor to finger impairment in chronic stroke. *Archives of Physical Medicine and Rehabilitation*, *87*(9), 1262–1269. https://doi.org/10.1016/j.apmr.2006.05.013
32. Araujo, R. S., Silva, C. R., Netto, S. P. N., Morya, E., & Brasil, F. L. (2021). Development of a Low-Cost EEG-Controlled Hand Exoskeleton 3D Printed on TextilesRommell. *Frontiers in Neuroscience*. https://doi.org/10.3389/fnins.2021.661569
33. Carlson, L. E., Veatch, B. D., & Frey, D. D. (1995). Efficiency of Prosthetic Cable and housing. *JPO Journal of Prosthetics and Orthotics*, *7*(3), 96–99. https://doi.org/10.1097/00008526-199500730-00006
34. Vergara, M., Agost, M. J., & Gracia-Ibáñez, V. (2017). Dorsal and palmar aspect dimensions of hand anthropometry for designing hand tools and protections. *Human Factors and Ergonomics in Manufacturing & Service Industries*, *28*(1), 17–28. https://doi.org/10.1002/hfm.20714

35. Vergara, M., Sancho-Bru, J. L., Gracia-Ibáñez, V., & Pérez-González, A. (2014). An introductory study of common grasps used by adults during performance of activities of Daily Living. *Journal of Hand Therapy*, *27*(3), 225–234. https://doi.org/10.1016/j.jht.2014.04.002
36. Francisco, G. E., & McGuire, J. R. (2012). Poststroke Spasticity Management. *Stroke*, *43*(11), 3132–3136. https://doi.org/10.1161/strokeaha.111.639831
37. The 90s Robot. (n.d.). Biomimetic Hand V2. GradCab.
38. Edwards, S. J., Buckland, D. J., & McCoy-Powlen, J. (2002). *Developmental & Functional hand grasps*. Slack.
39. Jiménez-Arberas, E., & Ordóñez-Fernández, F. F. (2021). Discontinuation or abandonment of mobility assistive technology among people with neurological conditions. Interrupción o abandono en el uso de productos de apoyo para la movilidad en personas con afectación neurológica. *Revista de neurologia*, *72*(12), 426–432. https://doi.org/10.33588/rn.7212.2020655
40. Safaz, I., Tok, F., Tugcu, I., Turk, H., Yasar, E., & Alaca, R. (2015). Use and abandonment rates of assistive devices/orthoses in patients with stroke. *Gulhane Medical Journal*, *57*(2). https://doi.org/10.5455/gulhane.152325
41. Feix, T., Romero, J., Schmiedmayer, H.-B., Dollar, A. M., & Kragic, D. (2016). The Grasp Taxonomy of Human Grasp Types. *IEEE Transactions on Human-Machine Systems*, *46*(1), 66–77. https://doi.org/10.1109/thms.2015.2470657
42. Delph, M. A., Fischer, S. A., Gauthier, P. W., Luna, C. H., Clancy, E. A., & Fischer, G. S. (2013). A Soft Robotic Exomusculature Glove with Integrated SEMG Sensing for Hand Rehabilitation. *2013 IEEE 13th International Conference on Rehabilitation Robotics (ICORR)*. https://doi.org/10.1109/icorr.2013.6650426
43. Gasser, B. W., Bennett, D. A., Durrough, C. M., & Goldfarb, M. (2017). Design and Preliminary Assessment of Vanderbilt Hand Exoskeleton. *2017 International Conference on Rehabilitation Robotics (ICORR)*. https://doi.org/10.1109/icorr.2017.8009466
44. Jian, E. K., Chan, Gouwanda, D., & Kok Kheng, T. (2018). Wearable Hand Exoskeleton for Activities of Daily Living. *2018 IEEE-EMBS Conference on Biomedical Engineering and Sciences (IECBES)*. https://doi.org/10.1109/iecbes.2018.8626719
45. Polygerinos, P., Galloway, K. C., Sanan, S., Herman, M., & Walsh, C. J. (2015). EMG controlled soft robotic glove for assistance during activities of Daily Living. *2015 IEEE International Conference on Rehabilitation Robotics (ICORR)*. https://doi.org/10.1109/icorr.2015.7281175
46. Llop-Harillo, I., Pérez-González, A., Starke, J., & Asfour, T. (2019). The Anthropomorphic Hand Assessment Protocol (AHAP). *Robotics and Autonomous Systems*, *121*, 103259. https://doi.org/10.1016/j.robot.2019.103259